




Preparation and characterization of form-stable tetradecanol–palmitic acid expanded perlite composites containing carbon fiber for thermal energy storage

Fei Cheng¹ · Yaoting Huang² · Ruilong Wen¹ · Xiaoguang Zhang¹  · Zhaohui Huang¹ · Minghao Fang¹ · Yan'gai Liu¹ · Xiaowen Wu¹ · Xin Min¹

Received: 12 March 2018 / Accepted: 18 September 2018 / Published online: 25 September 2018

© Akadémiai Kiadó, Budapest, Hungary 2018

Abstract

In this study, tetradecanol–palmitic acid/expanded perlite composites containing carbon fiber (TD-PA/EP-CF CPCMs) were prepared by a vacuum impregnation method. Binary eutectic mixtures of PA and TD were utilized as thermal energy storage material in the composites, where EP behaved as supporting material. X-ray diffraction demonstrated that crystal structures of PA, TD, EP, and CF remained unchanged, confirming no chemical interactions among raw materials besides physical combinations. The microstructures indicated that TD-PA was sufficiently absorbed into EP porous structure, forming no leakage even in molten state. Differential scanning calorimetry estimated the melting temperature of TD-PA/EP-CF CPCM to 33.6 °C, with high phase change latent heat (PCLH) of 138.3 kJ kg⁻¹. Also, the freezing temperature was estimated at 29.7 °C, with PCLH of 137.5 kJ kg⁻¹. The thermal cycling measurements showed that PCM composite had adequate stability even after 200 melting/freezing cycles. Moreover, the thermal conductivity enhanced from 0.48 to 1.081 W m⁻¹ K⁻¹ in the presence of CF. Overall, the proposed CPCMs look promising materials for future applications due to their appropriate phase change temperature, elevated PCLH, and better thermal stability.

Keywords Energy storage · Palmitic acid · Binary eutectic mixture · Carbon fiber · Thermal stability · Thermal conductivity

Introduction

Nowadays, energy depletion has become a major crisis worldwide, resulting in increased innovation of advanced energies storage devices. Phase change materials (PCMs) could be used for energy storage materials as they can absorb and release thermal energy during phase change. In view of this, PCMs become one of the most widely

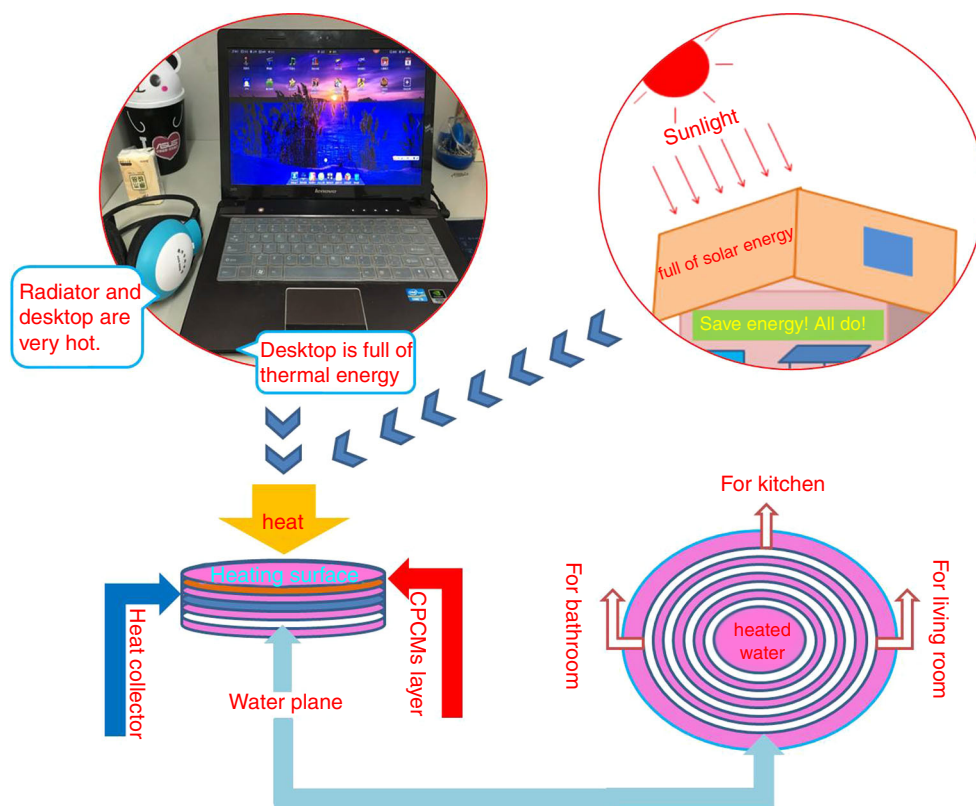
implemented materials in solar energy, energy conservation in buildings, thermal insulation, and thermal regulation due to their high thermal storage capacity [1–5]. However, as external wall materials of buildings are exposed to sun, solar energy can be absorbed by injecting PCMs with low melting temperatures into external wall materials. This principle also applies to computers, which can get very hot when working for long time. In this case, heat generated by the computer has enormous influence on operation of central processing unit; hence, many measures have been adopted to solve these issues, including installation of radiators and placing smaller fan under laptops. Most of these measures caused increasing energy consumption. Therefore, research related to PCMs applied to computers absorbing redundant thermal energy for cooling down is increasingly explored. The related application process is shown in Fig. 1. Several studies have shown that PCMs can solve the problem but PCMs require suitable phase change temperature (PCT) values slightly below 35 °C and high phase change latent heat (PCLH). In view of this, paraffin

✉ Zhaohui Huang
huang118@cugb.edu.cn

¹ Beijing Key Laboratory of Materials Utilization of Nonmetallic Minerals and Solid Wastes, National Laboratory of Mineral Materials, School of Materials Science and Technology, China University of Geosciences (Beijing), No. 29 Xueyuan Road, Haidian District, Beijing 100083, People's Republic of China

² School of Science, Beijing University of Posts and Telecommunications, Beijing 100876, People's Republic of China

Fig. 1 Schematic diagram of PCMs composites application in worktable and building



[6, 7], fatty acids [8, 9], polyhydric alcohols [10], and salt hydrate [11] were investigated.

Palmitic acid (PA) is a PCM-based polyhydric alcohol. PA has attracted many interests because of its high PCLH, non-corrosive, no separation of subcooling phase, and low price [12–14]. Owing to its possessing correlative high PCT, PA could not be directly applied at low temperatures, such as indoor and outdoor temperatures. Hence, to widen applications of PA in low-temperature surroundings, PCT should be lowered by mixing PA with other PCMs at certain ratios to form composite PCMs (CPCMs) [15–17]. These CPCMs could not only overcome the disadvantages of single PCMs but also can expand applications of PCMs.

Tetradecanol (TD) is potentially used in binary PCMs systems due to its excellent properties [18]. TD is a kind of paraffin PCM with high PCLH and low PCT with almost no supercooling phenomenon and phase separation, hence relevant in PCMs filed [19].

Perlite is an inert glassy volcanic rhyolitic rock that can be expanded up to 10–20 times its original volume when heated rapidly at 700–1200 °C [20]. Expanded perlite (EP) is classified as ultra-lightweight material and acts as an excellent insulator and porous matrix material [21–23]. In addition, EP is inexpensive and abundantly available, which could make it a feasible candidate for economical building materials for incorporating fatty acids like PCMs in thermal energy storage buildings. However, similar to

other porous materials, EP suffers from low thermal conductivity when prepared with phase change material. Therefore, materials with high thermal conductivities could be utilized to enhance the thermal conductivities of PCMs compounded with porous materials.

In this study, TD-PA/EP-CF CPCM was prepared by vacuum impregnation method. TD-PA composite acted as latent heat storage material and EP was utilized as TD-PA matrix. TD was mixed evenly with PA at ratio of 7:3. CF was added to the porous structure as high thermal conductivity material to improve thermal conductivity. The microstructure, chemical composition, crystal structure, and thermal properties were characterized by various methods. The formation of binary eutectic mixture and addition of CF yielded a stable TD-PA/EP-CF CPCM with more appropriate PCT, elevated PCHL, and better thermal conductivity than PCMs reported by others [27–29].

Experimental

Materials

Palmitic acid (PA, AR, m.p. 62.5–64.0 °C) was purchased from Sinopharm Chemical Reagent. Tetradecanol (TD, AR, m.p. 35.8–37.2 °C) was from Tianjin Guangfu Fine Chemical Research Institute. EP was obtained from Beijing

Bo stand Scientific Instruments, and CF was supplied by Shen Zhen Fiber Valley Technology.

Sample preparation

TD-PA CPCM was prepared by weighing TD and PA at ratios ranging from 10:0 to 0:10, which were then mixed evenly and stirred during the melting process. Next, TD-PA/EP-CPCM was synthesized by vacuum impregnation method. TD-PA in molten state was mixed with CF at ratio of 3 mass%. The mixture was then transferred to a drying oven and stirred evenly for 12 h at 80 °C to obtain a homogeneous mixture. And then, EP was added to the mixture and put in the vacuum drying oven under vacuum then taken out. The absorption process was repeated to yield the final TD-PA/EP-CPCM product. The preparation process is summarized in Fig. 2.

Characterization

The morphologies of the prepared CPCM were observed by scanning electronic microscopy (SEM, JSM-IT3000).

The crystal structures were examined by X-ray diffractometer (XRD, model XD-3). Solid–liquid phase change temperatures and latent heat capacities of PCMs composites were carried out by DSC instrument (DSC214Polyma) under nitrogen atmosphere at heating rate of 10 °C min⁻¹. The melting and freezing temperatures were obtained by drawing a line at the point of maximum slope in DSC peak. The latent heat was calculated by numerical integration of the peak using inherent software of DSC. The thermal stability of PCM composite was determined by America TA instruments Q5000. In each case, the specimen (about 10 mg) was heated from 25 to 700 °C at linear heating rate of 10 °C min⁻¹ under nitrogen atmosphere. The thermal conductivity was tested by XFA 500 instrument according to the standard test method by the flash method (ASTM E 1461-01).

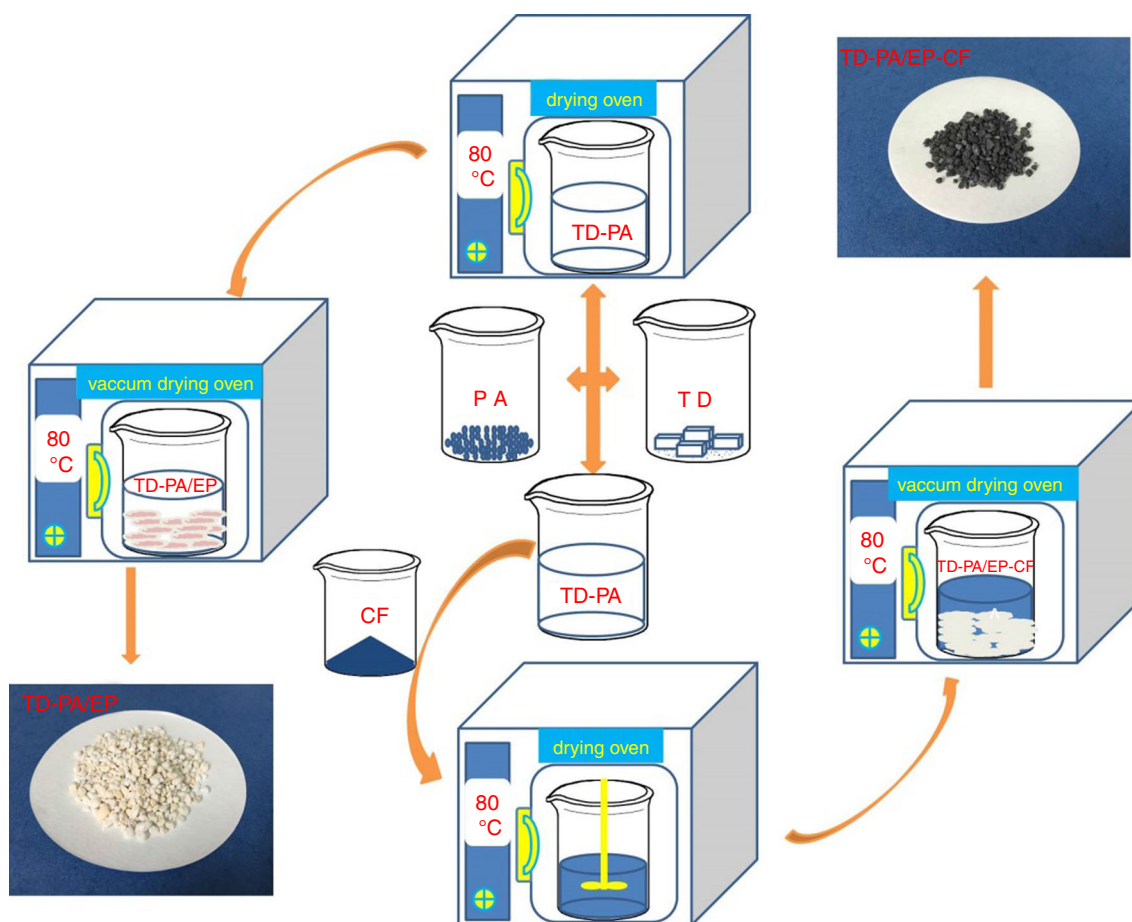


Fig. 2 Preparation process of TD-PA/EP and TD-PA/EP-CF composites

Results and discussion

XRD analysis

The XRD patterns of PA, EP, TD-PA/EP, CF, and TD-PA/EP-CF composites are depicted in Fig. 3a, where the peaks of PA are shown in black bottom curve. The curve of EP appeared smooth with no significant peaks. The curves of TD-PA/EP and TD-PA/EP-CF composites contained the main characteristic peaks of PA, revealing that the crystal structure of PA remained undestroyed. The relationship between CF, TD-PA/EP and TD-PA/EP-CF composites is illustrated in Fig. 3b. The primary peaks of TD-PA/EP composite were located at 21.7° and 23.6° while those of CF mainly appeared at 25.5°, 35°, 43°, and 57.5°. The latter resulted from the incomplete crystal structure formation. The peaks of TD-PA/EP-CF composites consisted of combined major peaks of both TD-PA/EP composite and CF, suggesting that the crystal structure remained unchanged. Also, no chemical interaction occurred among the materials.

Microstructure analysis

Figure 4 illustrates the SEM photographs of EP, TD-PA/EP, CF, TD-PA/EP-CF, and TD-PA/EP-CF composites. Also, appearance images of PA-TD/EP and TD-PA/EP-CF composite were taken at room temperature and after heating to 80 °C. Figure 4a represents EP, showing large numbers of pores with different sizes. On the other hand, TD-PA/EP composite revealed pores filled with PCMs (TD-PA composite) (Fig. 4b). The microstructure of CF appeared fibrous with different lengths, where shortest was about 45 μm (Fig. 4c). The microstructure of TD-PA/EP-

CF composite is shown in Fig. 4d. Some fibrous bars appeared when compared to Fig. 4b. On the other hand, the enlarged image clearly displayed the microstructure of TD-PA/EP-CF containing numerous fibrous bars (Fig. 4e), where TD-PA composite inlaid the porous structure of EP.

Figure 4f exhibits the microstructure of TD-PA/EP-CF composites after 200 times thermal cycles. The pores still covered with PCMs and CF bars. Figure 4g, h displays the optical images of, respectively, PA-TD/EP and TD-PA/EP-CF composites at room temperature and after heating at 80 °C. Both composites became glossed without apparent leakage trace, revealing that EP provided structural support to the composites and prevented leakage of PCMs during melting through capillary and surface tension forces.

Thermal properties

Figure 5 represents the diagram of TD-PA at ratios varying from 10:0 to 0:10 during melting and freezing processes, named as G1–G11, where G1 represents pure TD and G11 expresses pure PA. Pure TD melted at 36.6 °C with an enthalpy value of 201.9 J g⁻¹ while PA melted at 61.4 °C with an enthalpy value of 218 J g⁻¹. As TD-PA ratio decreased, the melting point and enthalpy value started to, respectively, reduce and increase until the ratio reached 7:3, the melting point and enthalpy values separately reached 33.4 °C and 213.9 J g⁻¹. Because TD-PA composite formed an eutectic mixture during this time, the melting point and enthalpy values were in an ideal state that the melting temperature got the lowest point and the enthalpy values were only lower than that of pure PA. And when TD-PA ratio increased, the melting point of TD-PA composite rose and two absorption heat peaks gradually appeared. Thus, TD-PA composite formed a stable eutectic

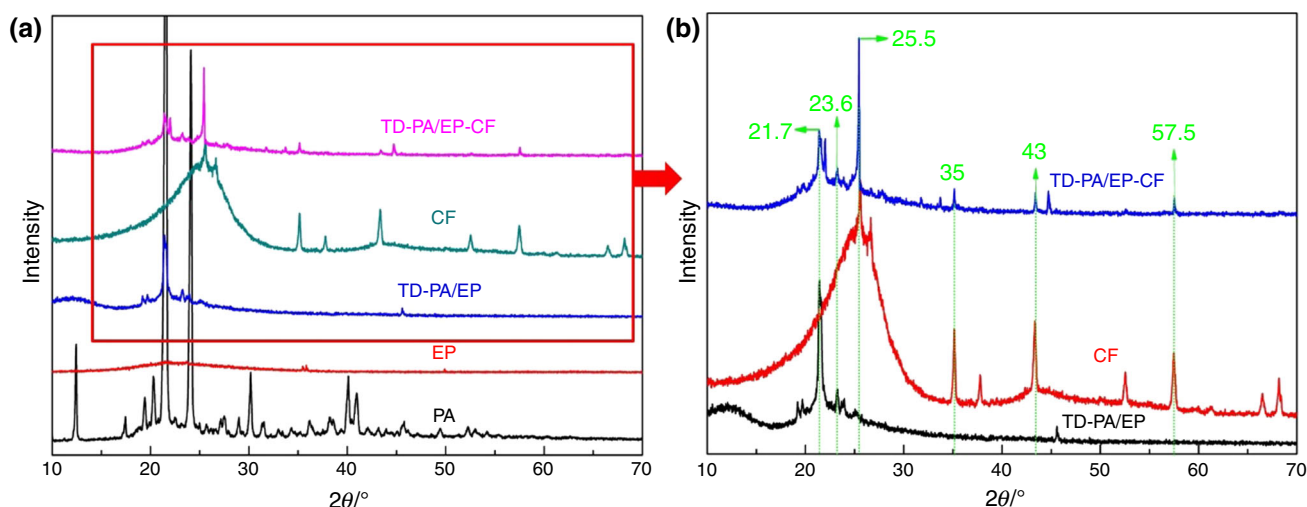


Fig. 3 XRD patterns of CPCMs. **a** PA, EP, TD-PA/EP, CF, and TD-PA/EP-CF composites. **b** TD-PA/EP, CF, and TD-PA/EP-CF composites

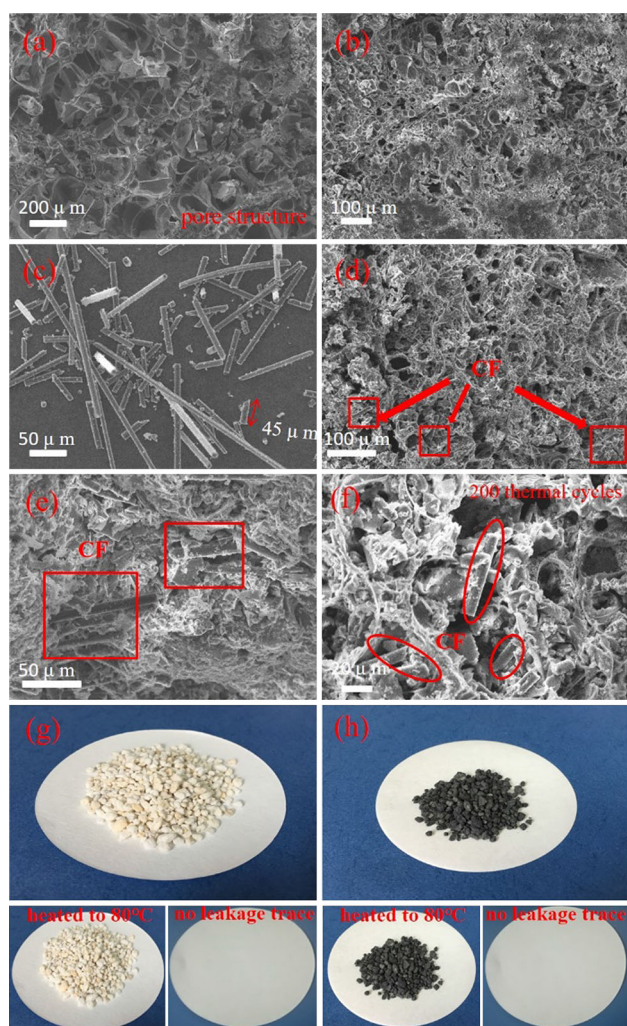


Fig. 4 SEM photographs of EP, TD-PA/EP, CF, TD-PA/EP-CF, TD-PA/EP-CF composites with greater enlargement and after 200 thermal cycles. Appearance of PA-TD/EP and PA-TD/EP-CF composites at room temperature and after heating at 80 °C, appearance of filter paper after absorbing the leaked PCMs

mixture with better thermal properties at mixture ratio of 7:3.

Figure 6a illustrates the DSC profiles of PA, PA/EP, TD-PA/EP, and TD-PA/EP-CF composites. Two overlap areas were noticed: one comprised of PA and PA/EP composites and the other TD-PA/EP and TD-PA/EP-CF composites. Slight differences between internal materials of both groups appeared. As depicted in Fig. 6a and Table 1, PA melted at 61.4 °C with PCLH of 218 J g⁻¹ while PA/EP composite with 40 mass% paraffin/expanded perlite melted at 61.0 °C by absorbing 144.3 J thermal energy per gram. TD-PA/EP composite melted at 33.2 °C with PCLH of 143 J g⁻¹. In addition, TD-PA/EP-CF

composite melted when heated to 33.6 °C with PCLH of 138.3 J g⁻¹. The combination of PCMs with supporting materials slightly changed the enthalpy value. Compared with PA and PA/EP composites, the enthalpy values of TD-PA and TD-PA/EP composites were smaller but melting points declined significantly. Compared to TD-PA/EP composite, TD-PA/EP-CF underwent a little change in enthalpy value when CF was added. Overall, CPCMs gained good thermal properties.

Figure 6b shows the DSC curves of TD-PA/EP-CF and TD-PA/EP-CF composites after 200 thermal cycles. Both PCT varied faintly from 33.6 to 33.1 °C and phase change enthalpy displayed small variation of about 1.4 J g⁻¹ after 200 thermal cycles. This indicated composites with near perfect thermal stability suitable for thermal energy storage applications.

Thermal stability

Thermogravimetry analysis (TG) and derivative thermogravimetry (DTG) measurements are critical in identifying the thermal stability of materials. Figure 7a represents the TG curves of PA/EP, TD-PA/EP, and TD-PA/EP-CF composites. The maximum mass loss and temperatures of maximum mass loss are gathered in Table 2. PA/EP composite started to dissolve at 193 °C that ended at 259.5 °C with recorded of 66.3% maximum mass loss. On the other hand, TD-PA/EP composite also dissolved when heated to 152.2 °C with 66.4% mass loss at end of the process. These mass losses were attributed to decomposition of PCMs. Similarly, TD-PA/EP-CF composite lost 63.6% of mass from 151.4 to 220.8 °C. However, the mass loss was small compared to those of PA/EP and TD-PA/EP composites. This was related to CF, which did not resolve with temperature range. Figure 7b indicates that thermal degradation temperature reduced gradually as the composite became more complex. The thermal degradation of PA/EP composite was recorded at 223.8 °C, while those of TD-PA/EP and TD-PA/EP-CF composites were 190.1 °C and 188.4 °C, respectively. The latter were comparatively high than indoor temperature. In sum, TD-PA/EP-CF composite containing PCM showed good thermal ability.

Thermal conductivity

Thermal conductivity is an important parameter in phase change material. As previously mentioned, TD-PA/EP CPCM with low thermal conductivity could increase the response time of melting and freezing of latent heats. Therefore, improving the thermal conductivity is important

Fig. 5 Diagram of TD-PA at ratios ranging from 10:0 to 0:10 during melting and freezing processes

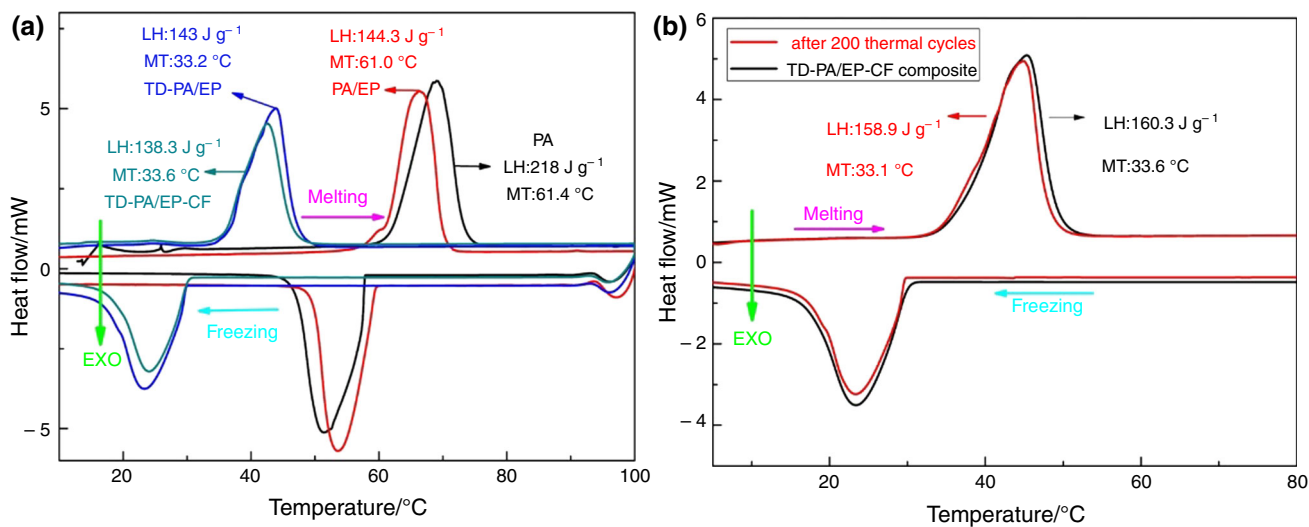
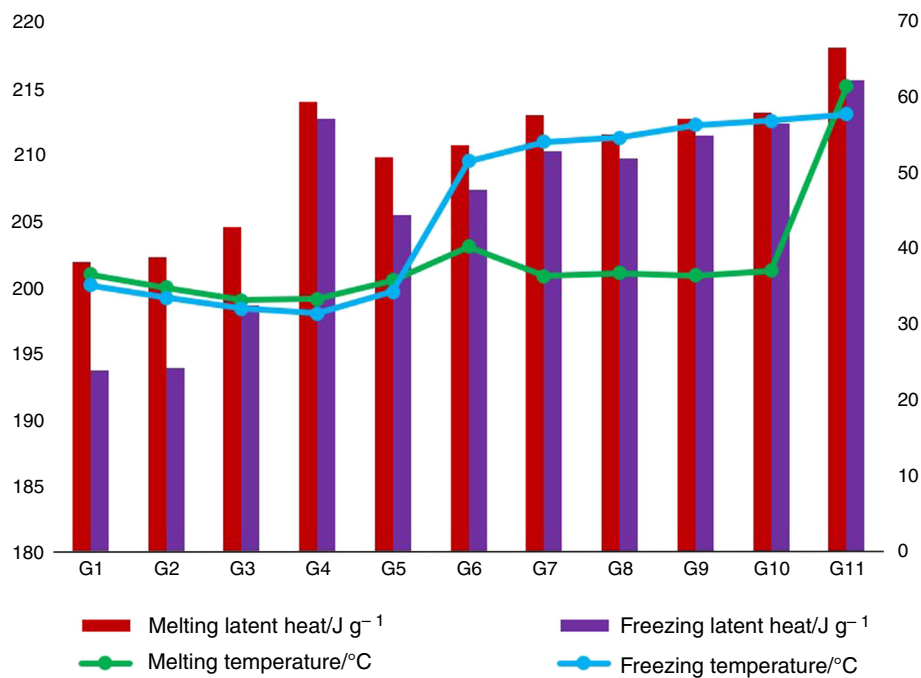


Fig. 6 DSC curves of **a** melting and freezing processes of PA, PA/EP, TD-PA/EP, and TD-PA/EP-CF composites and **b** melting and freezing processes of TD-PA/EP-CF composites after 200 thermal cycles

Table 1 Melting and freezing processes data of PA, PA/EP, TD-PA/EP, and TD-PA/EP-CF composites

Sample	Melting process		Freezing process	
	Temperature/°C	Latent heat/J g ⁻¹	Temperature/°C	Latent heat/J g ⁻¹
PA	61.4	218	57.8	215.6
PA/EP	61.0	144.3	59.5	143.9
TD-PA/EP	33.2	143	29.3	142.6
TD-PA/EP-CF	33.6	138.3	29.7	137.5

in materials design. Due to high thermal conductivity of CF, the thermal conductivities of the composites could subsequently be improved by adding CF. Hence, CF was selected to enhance the conductivity of PCM composites. The thermal diffusivity was measured by laser flash method, and thermal conductivity was calculated using Eq. (1) [24].

$$\lambda = \alpha \rho C_p \quad (1)$$

where λ is the thermal conductivity, α is thermal diffusivity, ρ is bulk density obtained using Archimedes method, and C_p is heat capacity measured by multiple curve method.

Figure 8 describes the thermal conductivities of PA/EP, TD-PA/EP, and TD-PA/EP-CF composites. The thermal conductivity of TD-PA/EP improved with addition of CF. The calculated thermal conductivities of TD-PA, TD-PA/EP, and TD-PA/EP-CF composites are given in Table 3. The thermal conductivity of TD-PA in solid state was estimated at $0.48 \text{ W m}^{-1} \text{ K}^{-1}$, while that of TD-PA/EP was only $0.463 \text{ W m}^{-1} \text{ K}^{-1}$. This indicated that EP reduced the thermal conductivity of TD-PA composite. However, as thermal conductivity of TD-PA/EP-CF rose to $1.081 \text{ W m}^{-1} \text{ K}^{-1}$, thermal conductivity enhanced by more than two folds in the presence of CF when compared to both TD-PA and TD-PA/EP composites. Hence, CF exhibited high thermal conductivity.

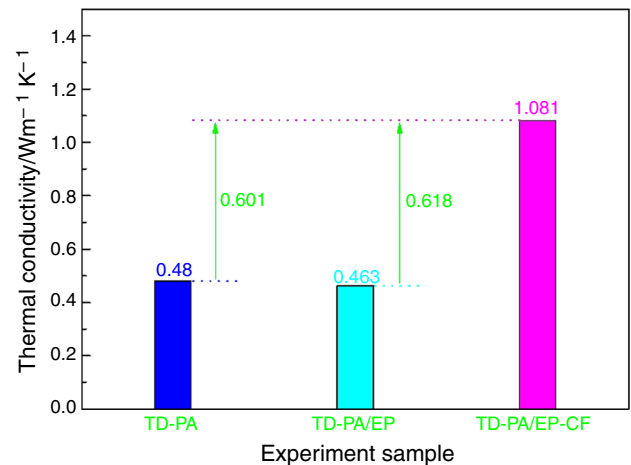


Fig. 8 Thermal conductivities of PA/EP, TD-PA/EP, and TD-PA/EP-CF composites

Table 4 presents the thermal properties and conductivities of TD-PA/EP-CF CPCM in comparison with PCMs found in the literature. The prepared TD-PA/EP-CF CPCM demonstrated relatively high thermal enthalpy, as well as suitable temperature and thermal conductivity. Therefore, TD-PA/EP-CF CPCM demonstrated potential for thermal energy storage systems.

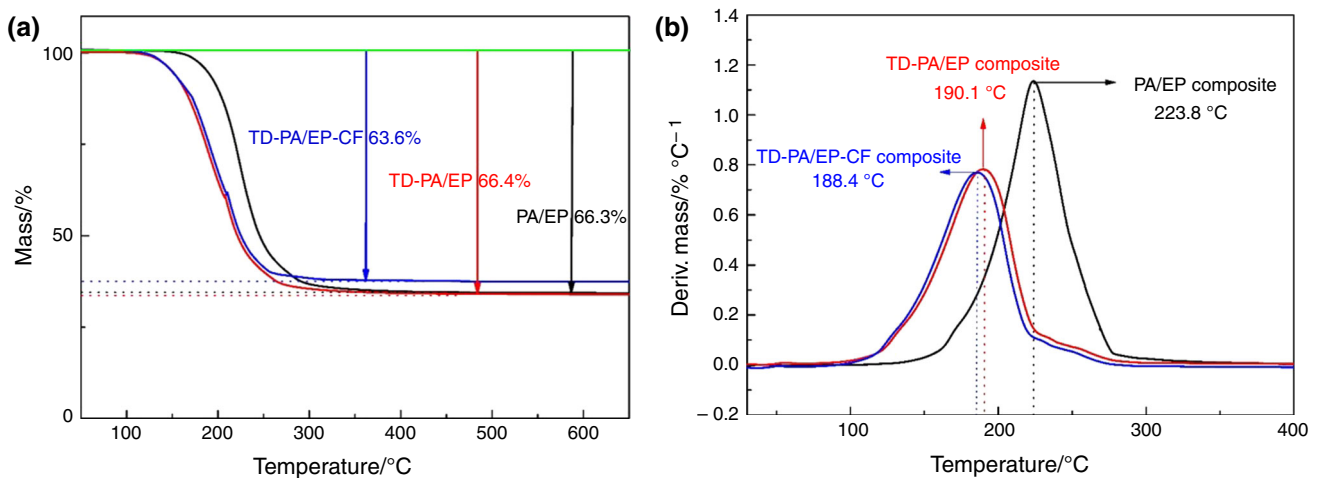


Fig. 7 a TG and b DTG curves of PA/EP, TD-PA/EP, and TD-PA/EP-CF composites

Table 2 TG and DTG data of PA/EP, TD-PA/EP, and TD-PA/EP-CF composites

Experiment sample	Temperature of mass loss/°C			Maximum mass loss/%
	Beginning	Thermal degradation	Finishing	
PA/EP	193	223.8	259.5	66.3
TD-PA/EP	152.2	190.1	221.6	66.4
TD-PA/EP-CF	151.4	188.4	220.8	63.6

Table 3 Thermal conductivity values of PA/EP, TD-PA/EP, and TD-PA/EP-CF composites

Sample	$\alpha \times 10^{-6}/\text{m}^2 \text{ s}^{-1}$	$\rho \times 10^3/\text{kg m}^{-3}$	$C_p \times 10^3/\text{J kg}^{-1} \text{ K}^{-1}$	$\lambda/\text{W m}^{-1} \text{ K}^{-1}$
TD-PA	0.338	1.247	1.14	0.48
TD-PA/EP	0.332	1.235	1.13	0.463
TD-PA/EP-CF	0.901	1.026	1.17	1.081

Table 4 Comparison of thermal properties and conductivities of prepared CPCMs with those of CPCMs found in the literature

Sample	Melting process		Freezing process		Thermal conductivity/ $\text{W m}^{-1} \text{ K}^{-1}$	References
	Temperature/ $^{\circ}\text{C}$	Latent heat/ J g^{-1}	Temperature/ $^{\circ}\text{C}$	Latent heat/ J g^{-1}		
Expanded perlite/ <i>n</i> -eicosane/carbon nanotubes (1 mass%)	36.12	157.43	35.5	157.43	0.32	[25]
Palmitic acid– TiO_2 (5 mass%) composite	61.59	180.03	–	–	0.35	[26]
Capric–palmitic/expanded perlite composite	25.7	88.39	–	–	0.2759	[27]
Lauric–palmitic–stearic acid/expanded perlite composite	31.8	81.5	30.3	81.3	0.44	[28]
Palmitic acid/polypyrrole composites	59.9	166.3	58.8	170.7	–	[14]
40 mass% paraffin/expanded perlite composite	27.6	54.8	24.1	54	0.37	[29]
TD-PA/EP composite	33.2	143	29.3	142.6	0.463	Present
TD-PA/EP-CF composite	33.6	138.3	29.7	137.5	1.081	Present

Conclusions

The preparation and characterization of TD-PA/EP-CF CPCMs as solar and thermal energy storage materials were reported. TD-PA composite at ratio of 7:3 formed binary eutectic mixture, with low melting point and proper PCLH. In TD-PA/EP-CF composite, TD-PA acted as CPCMs for thermal energy storage and EP as supporting material. Due to capillary and surface tension forces, TD-PA could uniformly be dispersed in EP without chemical interaction. Hence, CF was used to enhance the thermal conductivity values of CPCMs. The crystal structure of TD, PA, and EP remained unchanged in the composite material as verified by XRD. Also, TD-PA was sufficiently absorbed in EP porous structure, with no leakage even in molten state as confirmed by SEM. TD-PA/EP-CF composite melted at 33.6°C with high PCLH of 138.3 kJ kg^{-1} and froze at 29.7°C with PCLH of 137.5 kJ kg^{-1} . On the other hand, thermal cycling measurements showed PCM composite to have adequate stability even after 200 melting/freezing cycles. Moreover, its thermal conductivity enhanced from 0.48 to $1.081 \text{ W m}^{-1} \text{ K}^{-1}$ in the presence of CF. Therefore, CPCMs (TD-PA/EP-CF composite) would have great prospects in solar energy utilization, computers, indoor cooling instruments as thermal energy storage materials with appropriate PCT, high PCLH, and better thermal stability.

Acknowledgements This work was financially supported by the Fundamental Research Funds for the Central Universities for financial support (Grant Nos. 2652017361), the National Key Laboratory Open Fund (Grant Nos. 10042015003) and the National Natural Science Foundations of China (Grant Nos. 51472222, 51872268).

References

1. Yu S, Wang X, Wu D. Microencapsulation of *n*-octadecane phase change material with calcium carbonate shell for enhancement of thermal conductivity and serving durability: synthesis, microstructure, and performance evaluation. *Appl Energy*. 2014;114:632–43.
2. Huang J, Wang T, Zhu P, Xiao J. Preparation, characterization, and thermal properties of the microencapsulation of a hydrated salt as phase change energy storage materials. *Thermochim Acta*. 2013;557:1–6.
3. Wen RL, Huang ZH, Huang YT, Zhang XG, Min X, Fang MH, Liu YG, Wu XW. Synthesis and characterization of lauric acid/expanded vermiculite as form-stabilized thermal energy storage materials. *Energy Build*. 2016;116:677–83.
4. Zhang XG, Liu HT, Huang ZH, et al. Preparation and characterization of the properties of polyethylene glycol@ Si_3N_4 nanowires as phase-change materials. *Chem Eng J*. 2016;301:229–37.
5. Cheng F, Wen RL, Huang ZH, Fang MH, Liu YG, Wu XW, Min X. Preparation and analysis of lightweight wall material with expanded graphite (EG)/paraffin composites for solar energy storage. *Appl Therm Eng*. 2017;120:107–14.
6. Yang D, Shi S, Xiong L, et al. Paraffin/palygorskite composite phase change materials for thermal energy storage. *Sol Energy Mater Sol Cells*. 2016;144:228–34.
7. Chen Z, Cao L, Fang G, Shan F. Synthesis and characterization of microencapsulated paraffin microcapsules as shape-stabilized

- thermal energy storage materials. *Nanoscale Microscale Thermophys Eng.* 2013;17(2):112–23.
8. Fauzi H, Metselaar HSC, Mahlia TMI, et al. Preparation and thermal characteristics of eutectic fatty acids/*Shorea javanica* composite for thermal energy storage. *Appl Therm Eng.* 2016;100:62–7.
 9. Fu X, Liu Z, Wu B, et al. Preparation and thermal properties of stearic acid/diatomite composites as form-stable phase change materials for thermal energy storage via direct impregnation method. *J Therm Anal Calorim.* 2016;123(2):1173–81.
 10. Sarı A, Alkan C, Biçer A. Synthesis and thermal properties of polystyrene-graft-PEG copolymers as new kinds of solid–solid phase change materials for thermal energy storage. *Mater Chem Phys.* 2012;133(1):87–94.
 11. Wu Y, Wang T. The dependence of phase change enthalpy on the pore structure and interfacial groups in hydrated salts/silica composites via sol-gel. *J Colloid Interface Sci.* 2015;448:100–5.
 12. Mehrali M, Latibari ST, Mehrali M, Mahlia TMI, Sadeghinezhad E, Metselaara HSC. Preparation of nitrogen-doped graphene/palmitic acid shape stabilized composite phase change material with remarkable thermal properties for thermal energy storage. *Appl Energy.* 2014;135:339–49.
 13. Zhang N, Yuan YP, Du YX, Cao XY, Yuan YG. Preparation and properties of palmitic-stearic acid eutectic mixture/expanded graphite composite as phase change material for energy storage. *Energy.* 2014;78:950–6.
 14. Silakhorla M, Metselaara HSC, Mahliab TMI, Fauzia H, Baradarana S, Naghavia MS. Palmitic acid/polypyrrole composites as form-stable phase change materials for thermal energy storage. *Energy Convers Manag.* 2014;80:491–7.
 15. Yuan YP, Zhang N, Li TY, et al. Thermal performance enhancement of palmitic-stearic acid by adding graphene nanoplatelets and expanded graphite for thermal energy storage: a comparative study. *Energy.* 2016;97:488–97.
 16. Zhang H, Gao XN, Chen CX, et al. A capric–palmitic–stearic acid ternary eutectic mixture/expanded graphite composite phase change material for thermal energy storage. *Compos Part A Appl Sci Manuf.* 2016;87:138–45.
 17. Li M, Wu ZS, Kao HT. Study on preparation, structure and thermal energy storage property of capric–palmitic acid/attapulgitite composite phase change materials. *Appl Energy.* 2011;88(9):3125–32.
 18. Zeng JL, Gan J, Zhu FR, Yu SB, Xiao ZL, et al. Tetradecanol/expanded graphite composite form-stable phase change material for thermal energy storage. *Sol Energy Mater Sol Cells.* 2014;127:122–8.
 19. Zuo JG, Li WZ, Weng LD. Thermal properties of lauric acid/1-tetradecanol binary system for energy storage. *Appl Therm Eng.* 2011;31:1352–5.
 20. Sengul O, Azizi S, Karaosmanoglu F, Tasdemir MA. Effect of expanded perlite on the mechanical properties and thermal conductivity of lightweight concrete. *Energy Build.* 2011;43(2):671–6.
 21. Karaipeklin A, Sarı A. Capric–myristic acid/expanded perlite composite as form-stable phase change material for latent heat thermal energy storage. *Renew Energy.* 2008;33(12):2599–605.
 22. Sarı A, Karaipeklin A. Preparation, thermal properties and thermal reliability of capric acid/expanded perlite composite for thermal energy storage. *Mater Chem Phys.* 2008;109(2):459–64.
 23. Sarı A, Karaipeklin A, Alkan C. Preparation, characterization and thermal properties of lauric acid/expanded perlite as novel form-stable composite phase change material. *Chem Eng J.* 2009;155(3):899–904.
 24. Latibari ST, Mehrali M, Mahlia TMI, Metselaar HSC. Fabrication and performances of microencapsulated palmitic acid with enhanced thermal properties. *Energy Fuels.* 2015;29(2):1010–8.
 25. Karaipekli A, Bicer A, Sari A, Tyagi VV. Thermal characteristics of expanded perlite/paraffin composite phase change material with enhanced thermal conductivity using carbon nanotubes. *Energy Convers Manag.* 2017;134:373–81.
 26. Sharma RK, Ganesan P, Tyagi VV, Metselaar HSC, Sandaran SC. Thermal properties and heat storage analysis of palmitic acid-TiO₂ composite as nano-enhanced organic phase change material (NEOPCM). *Appl Therm Eng.* 2016;99:1254–62.
 27. Zhang JW, Guan XM, Song XX, Hou HH, Yang ZP, Zhu JP. Preparation and properties of gypsum based energy storage materials with capric acid–palmitic acid/expanded perlite composite PCM. *Energy Build.* 2015;92:155–60.
 28. Zhang N, Yuan YP, Yuan YG, Li TY, Cao XL. Lauric–palmitic–stearic acid/expanded perlite composite as form-stable phase change material: preparation and thermal properties. *Energy Build.* 2014;82:505–11.
 29. Lu ZY, Zhang JR, Sun GX, Xu BW, Li ZJ, Gong CC. Effects of the form-stable expanded perlite/paraffin composite on cement manufactured by extrusion technique. *Energy.* 2015;82:43–53.